Quantum Chemical Study of the Thermal Decomposition of *o*-Quinone Methide (6-Methylene-2,4-cyclohexadien-1-one)

Gabriel da Silva and Joseph W. Bozzelli*

Department of Chemistry and Environmental Science, New Jersey Institute of Technology, Newark, New Jersey 07102

Received: May 1, 2007; In Final Form: June 11, 2007

o-Quinone methide (*o*-QM), or 6-methylene-2,4-cyclohexadiene-1-one, has been identified as an important intermediate in lignin and alkyl benzene combustion, and the thermal decomposition of *o*-QM is therefore relevant to the combustion of transportation fuels (which contain toluene) and of biomass and low-rank coals (which contain lignin). We present a comprehensive reaction mechanism for the unimolecular conversion of *o*-QM to the reaction intermediates tropone and fulvene, calculated using theoretical quantum chemical techniques. Enthalpies of formation for all reactants, products, and intermediates are calculated using the CBS-QB3 theoretical method. Transition states are determined with the CBS-QB3 method, which we use to obtain rate constants as a function of temperature from transition-state theory, with Wigner tunneling corrections applied to hydrogen-shift reactions. Barrier heights are also calculated with the BB1K density functional theory (DFT) method for thermochemical kinetics. Reaction pathways are identified leading to tropone (which rapidly decomposes to benzene + CO) and to fulvene + CO, via initial hydrogen transfer to 2-hydroxyphenylcarbene and via ring opening to 1,3,5,6-heptatetraen-1-one, respectively. Quantum Rice−Ramsperger−Kassel (QRRK) theory analysis of the reaction kinetics indicates that the dominant reaction pathway is formation of tropone via 2-hydroxyphenylcarbene; the formation of fulvene + CO via initial ring opening constitutes a secondary pathway, which becomes more important with increasing temperature. Our calculations, using BB1K barrier heights, yield the rate equation $k(T)$ [s^{-1}] = 2.64×10^{14} exp(−35.9/T [K]) for *o*-QM decomposition, which is in relatively good agreement with the experimental rate equation. Calculations provide an apparent activation energy of 71.3 kcal mol^{-1}, versus 67.2 kcal mol^{-1} from experiment.

Introduction

The quinone methides (*o*- and *p*-quinone methide and their substituted derivatives) are highly electrophilic and are known to act as DNA alkylating and cross-linking agents,[1] and considerable effort has been directed toward better understanding their properties and reaction mechanisms.[2] *o*-Quinone methide (*o*-QM) is also emerging as an important intermediate in the combustion of transportation fuels and in the pyrolysis of wood and low-rank coals.

A recent theoretical study of the reaction of the 2-methylphenyl radical with O_2 predicted *o*-QM formation to be a major reaction pathway, following the reactions of Scheme 1.[3] It was proposed that *o*-QM would be a significant intermediate during alkyl benzene combustion, especially for toluene and xylene.[3] Methyl *o*-quinone methides and other substituted derivatives may also be important in aromatic combustion processes. In Scheme 1 we demonstrate a potential pathway leading to *o*-QM formation from the reaction of the benzyl radical with O_2, which may also be important in toluene combustion (however, we also envisage a reaction leading to the 2-hydroxybenzoxyl radical which may proceed with a lower barrier). Furthermore, *o*-QM has been proposed as an intermediate in the reaction of the peroxy radical (HO_2) with the benzyl radical in the ortho position,[4] which should be significant in atmospheric processes and low-temperature combustion systems. This reaction process is illustrated in Scheme 2.[4] Alternatively, *o*-QM formation may react through a stepwise process, via OH dissociation in 1-hydroperoxy-2-methylene-3,5-cyclohexadiene (the product of benzyl + HO_2 addition), followed by loss of H.

SCHEME 1: Reaction Pathways for *o*-QM Formation from the 2-Methylphenyl + O_2 and Benzyl + O_2 Reactions

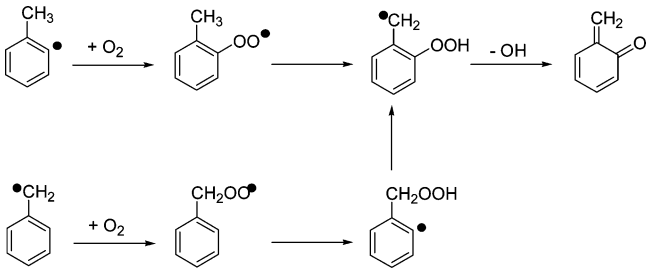

SCHEME 2: Reaction Pathways for *o*-QM Formation from the Benzyl + HO_2 Reaction[a]

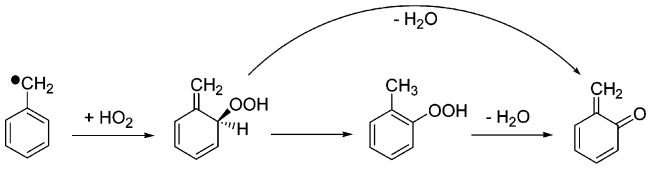

[a] Reactions according to Skokov et al.[4]

In addition to its formation in the combustion of aromatic fuels, *o*-QM has been proposed as an intermediate in the pyrolysis of lignin (wood) and low-rank coals. Chroman, a lignin

* To whom correspondence should be addressed. Phone: + 1 973 596 3459. Fax: +1 973 596 3586. E-mail: bozzelli@njit.edu.

10.1021/jp073335c CCC: $37.00
Published on Web 07/24/2007

SCHEME 3: Reaction Pathway for *o*-QM Formation from Chroman Pyrolysis

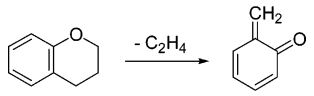

model compound, has been experimentally shown to decompose to *o*-QM + ethene (C_2H_4), as depicted in Scheme 3.[5−8] This reaction proceeds with an activation energy of 62.9 kcal mol^{-1}, and conversion of chroman to *o*-QM (or further decomposition products) is quantitative at temperatures of around 900 K and greater.[5,6] Two processes have been proposed for chroman decomposition:[5] (i) a two-step mechanism, where chroman opens to a diradical intermediate by C−C or more likely C−O bond cleavage, followed by dissociation of C_2H_4, and (ii) a concerted retro-Diels−Alder dissociation reaction. The correct reaction mechanism has not, to our knowledge, been elucidated.

As shown above, *o*-QM is an important intermediate in the thermal reactions of aromatic compounds, wood, and coal. Additionally, *o*-QM also occurs as an intermediate in the decomposition of *o*-hydroxybenzyl alcohol,[9] *o*-hydroxyphenylcarbene,[10] and 1,4-benzodioxin,[8] with similar quinone methides occurring as intermediates in the reactions of dibenzo-1,4-dioxins.[11] Experimentally, the pyrolysis of *o*-QM produces benzene + CO, with small amounts of fulvene. Trace amounts of acetylene and 1-buten-3-yne have also been detected, in a near one-to-one ratio. The rate constant for decomposition of *o*-QM has been measured as eq 1 [5] (in units of K and s^{-1}), where the activation energy is 67.2 kcal mol^{-1}. This rate constant was obtained over the narrow temperature range of ca. 850−1050 K.

$$k = 6.31 \times 10^{14} \exp(-33.8/T) \qquad (1)$$

o-Quinone methide occurs in a variety of important combustion and pyrolysis processes, and it is of value to understand its decomposition pathways and the thermochemistry of these reactions. In this study we use theoretical quantum chemical techniques to examine the mechanism and kinetics of *o*-QM decomposition. Reaction pathways are proposed leading to the known reaction products of *o*-QM pyrolysis, with thermochemical properties and reaction rate parameters calculated for all species and reactions, respectively. The results of this study identify the important reaction pathways for *o*-QM decomposition and provide rate constants for use in constructing kinetic models for the pyrolysis and combustion of, for example, toluene and lignin.

Computational Methods

All species identified on the *o*-QM potential energy surface are studied using the CBS-QB3 composite theoretical method.[12] The CBS-QB3 method requires an initial B3LYP/6-311G-(2d,d,p) geometry and frequency calculation and then uses the obtained molecular geometry for higher level energy corrections with the CCSD(T) and MP4 theoretical methods, followed by an extrapolation to the complete basis set (CBS) limit. From the CBS-QB3 calculations we determine enthalpies of formation using atomization reactions, with enthalpies of formation at 298 K of 52.103, 171.435, and 59.567 kcal mol^{-1} for H, C, and O, respectively.[13] Entropy ($S°_{298}$) and heat capacity ($C_p(T)$) values are determined for all species from principles of statistical mechanics using the SMCPS program,[14] with B3LYP/6-311G-(2d,d,p) geometries, frequencies, and moments of inertia. Entropy calculations take into account molecular symmetry, optical isomers, and the number of unpaired electrons. All ab initio and density functional theory calculations were performed using Gaussian 03.[15] CBS-QB3 enthalpies, geometries, frequencies, and moments of inertia for all species are listed as Supporting Information.

Transition states connecting each of the ground-state species have been identified using the CBS-QB3 theoretical method. All calculated transition states possessed a single imaginary frequency, where the mode of vibration connected the proposed reactants and products. In cases where the reactants and/or products obtained from a transition state were ambiguous, scans of the intrinsic reaction coordinate were performed. Rate contants, $k(T)$, were calculated between 300 and 2000 K for all reactions from conventional transition-state theory. Rate constants were empirically fit to the form $k(T) = A'T^n \exp(-E_a/RT)$. Reactions involving an intramolecular hydrogen shift were corrected for hydrogen tunneling through the potential energy barrier according to the Wigner formalism (eq 2).[16] Here, $\kappa(T)$ is the tunnelling correction, $\upsilon^{\ddagger}$ is the transition state's imaginary vibrational frequency, k_B is the Boltzmann constant and h is the Planck constant. After correcting $k(T)$ values for hydrogen

TABLE 1: Name, Structure, and Enthalpy of Formation ($\Delta_f H°_{298}$, kcal mol^{-1}) for All Products, Reactants, and Intermediates Considered in the Thermal Decomposition of *o*-QM

Structure	Name and Enthalpy (kcal mol^{-1})
	(1) *ortho*-quinone methide $\Delta_f H°_{298}$ = 16.4 (CBS-QB3) $\Delta_f H°_{298}$ = 12.8 (ref 3)
	(2) 2-hydroxyphenylcarbene $\Delta_f H°_{298}$ = 61.3 (CBS-QB3)
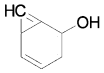	(3) bicyclo[4.1.0]hepta-2,4,7-trien-2-ol $\Delta_f H°_{298}$ = 71.9 (CBS-QB3)
	(4) 1,2,4,6-cycloheptatetraen-1-ol $\Delta_f H°_{298}$ = 55.5 (CBS-QB3)
	(5) tropone $\Delta_f H°_{298}$ = 18.3 (CBS-QB3)
	(6) 1,3,5,6-heptatetraen-1-one $\Delta_f H°_{298}$ = 62.0 (CBS-QB3)
	(7) 3,6-cycloheptadien-1-one-3,5-yl diradical $\Delta_f H°_{298}$ = 80.9 (CBS-QB3)
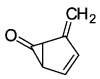	(8) 4-methylene-bicyclo[3.1.0]hex-2-en-6-one $\Delta_f H°_{298}$ = 49.6 (CBS-QB3)
	(9) fulvene $\Delta_f H°_{298}$ = 55.3 (CBS-QB3) $\Delta_f H°_{298}$ = 53.6 (ref 25)
	(10) bicyclo[3.2.0]hepta-3,5-dien-1-one $\Delta_f H°_{298}$ = 46.5 (CBS-QB3)
	(11) spiro[2.4]hepta-4,6-dien-1-one $\Delta_f H°_{298}$ = 49.7 (CBS-QB3)

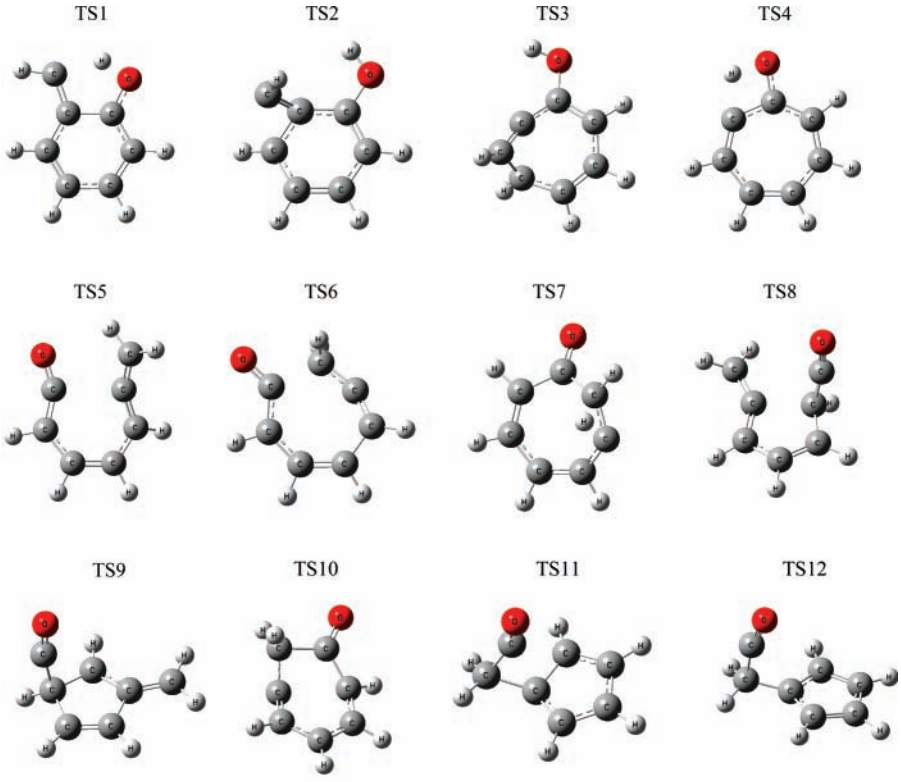

Figure 1. Transition-state geometries for all identified reactions in the thermal decomposition of *o*-QM, at the CBS-QB3 level. (Structure parameters are in Supporting Information).

tunneling, the A' and n parameters for these reactions were re-evaluated according to a least-squares error minimization in ln k. In addition to the CBS-QB3 calculations, transition states were also studied at the BB1K/6-31+G(2d,p) density functional theory (DFT) level, to provide a second determination of all barrier heights. The BB1K hybrid DFT method was developed for accurate thermochemical kinetics[17] and has recently been evaluated as one of the more accurate computational methods for barrier height calculations (with a mean unsigned error of 1.70 kcal mol^{-1} for the DBH24 barrier height test set, when using the 6-31+G(d,p) basis set).[18]

$$\kappa(T) = 1 + \frac{1}{24}\left(\frac{h\upsilon^{\ddagger}}{k_B T}\right) \qquad (2)$$

Modeling of the *o*-QM isomerization and unimolecular dissociation reactions is performed using QRRK theory with the modified strong collision model, as implemented in the CHEMDIS program.[19] This code makes use of a reduced set of three vibrational frequencies to describe the temperature dependence of C_p.[20] Molecules that proceed over the first reaction barrier in any given mechanism are thereafter considered to be chemically activated and may undergo further isomerization and/or dissociation reactions, reverse reaction back to *o*-QM, or stabilization by collision(s) with the bath gas (N_2). Reported rate constants are at a pressure of 1 atm (the pressure for the comparative experiments is not specified); calculated rate constants show little pressure fall-off down to 1×10^{-4} atm.

Results and Discussion

We find that the thermal decomposition of *o*-QM proceeds through the intermediate species tropone and fulvene (+CO). Fulvene is a known product of *o*-QM pyrolysis and should decompose further to benzene and to acetylene + 1-buten-3-yne. Tropone will also react to form benzene, by eliminating CO. This process should be rapid with respect to formation of tropone from *o*-QM and is therefore not considered here. In this section we discuss the potential reaction pathways leading to the production of these intermediates (all structures are identified in Table 1). In the following sections we will calculate thermochemical properties for all species involved in these reaction schemes and rate parameters for all reactions. Finally, we will use these calculated thermochemical and kinetic properties to model the decomposition kinetics of *o*-QM. Numerous other reaction pathways were considered during the course of this study but were eliminated due to prohibitively high barriers.

In our first reaction scheme (Scheme 4) we consider the formation of tropone via a hydroxyphenylcarbene intermediate. Initially, *o*-QM undergoes an intramolecular hydrogen shift to produce 2-hydroxphenylycarbene in a concerted process. The carbene group undergoes intramolecular addition to the aromatic ring at the ortho position, forming a bicyclic compound (bicyclo-[4.1.0]hepta-2,4,7-trien-2-ol). This species then opens to 1,2,4,6-cycloheptatetraen-1-ol, a seven-membered ring alcohol. A final intramolecular hydrogen shift from the OH group in 1,2,4,6-cycloheptatetraen-1-ol produces tropone. The rearrangement of phenylcarbenes to give seven-membered ring products is well-known in the literature.[21]

Golden and Jones[10] studied the reactions of the hydroxyphenylcarbenes and found that 3- and 4-hydroxyphenylcarbene reacted to predominantly yield tropone (31%) and 2-cresol (27%), where 2-cresol is proposed as a product of hydrogen abstraction by *o*-QM. A reaction scheme explaining the formation of *o*-QM from hydroxyphenylcarbene was presented, in which reaction proceeded via a benzooxetene intermediate

TABLE 2: Entropy ($S°_{298}$) and Heat Capacity ($C_p(T)$) Values for All Products, Reactants, and Intermediates Considered in the Thermal Decomposition of *o*-QM, at the B3LYP/6-311G(2d,d,p) Level[a]

species	$S°_{298}$	C_p(300)	C_p(400)	C_p(500)	C_p(600)	C_p(800)	C_p(1000)	C_p(1500)
1	79.91	27.08	35.09	41.79	47.20	55.14	60.63	68.70
2	78.35	26.66	34.90	41.80	47.36	55.47	61.01	69.03
3	82.44	28.52	36.76	43.42	48.63	56.03	61.03	68.35
4	79.54	27.95	36.40	43.49	49.10	56.94	61.98	69.00
5	78.93	26.29	34.18	40.94	46.46	54.64	60.30	68.56
6	90.89	31.32	38.38	44.20	48.93	56.08	61.20	68.94
7	82.69	28.51	36.34	42.88	48.15	55.91	61.28	69.13
8	81.46	27.52	35.90	42.72	48.08	55.83	61.15	68.96
9	69.90	21.26	28.28	34.12	38.79	45.63	50.41	57.60
10	80.26	26.27	34.79	41.84	47.43	55.50	61.00	68.97
11	81.14	27.73	36.05	42.85	48.20	55.92	61.21	68.98

[a] Species numbering corresponds to that of Table 1. All values in units of cal mol^{-1} K^{-1}.

TABLE 3: Rate Parameters (E_a, A', n) for Forward (for.) and Reverse (rev.) Reactions in the Thermal Decomposition of *o*-QM, from CBS-QB3 Calculations[a]

reaction	E_a(for.)	A'(for.)	n(for.)	E_a(rev.)	A'(rev.)	n(rev.)
1 → 3 (TS2)	69.3 (67.1)[b]	7.01×10^{11}	0.536	13.8 (11.6)[b]	1.94×10^{12}	0.107
3 → 4 (TS3)	3.4 (3.5)	2.28×10^{12}	0.101	19.9 (19.9)	3.65×10^{14}	−0.493
4 → 5 (TS4)	20.2 (18.4)	2.95×10^{16}	−1.323	57.5 (55.6)	7.12×10^{13}	−0.197
1 → 6 (TS5)	53.2 (54.8)	7.12×10^{11}	0.679	7.5 (9.2)	1.11×10^{11}	−0.021
6 → 7 (TS6)	28.3 (29.2)	8.78×10^{10}	−0.132	9.4 (10.3)	1.37×10^{12}	0.158
7 → 5 (TS7)	19.1 (16.8)	3.44×10^{13}	−0.293	81.8 (79.4)	1.18×10^{13}	0.258
6 → 8 (TS8)	29.8 (30.8)	6.67×10^{10}	0.336	42.2 (43.2)	1.19×10^{12}	0.719
8 → 9 + CO (TS9)	29.1 (29.2)	1.69×10^{12}	0.375			
6 → 10 (TS10)	31.5 (30.8)	1.25×10^{11}	−0.288	47.1 (46.3)	1.25×10^{12}	0.324
10 → 11 (TS11)	15.0 (10.7)	9.97×10^{11}	0.329	11.8 (7.5)	2.65×10^{12}	0.054
11 → 9 + CO (TS12)	14.9 (13.9)	5.57×10^{12}	0.144			

[a] Units: kcal, mol, and s. $k = A'T^n \exp(-E_a/RT)$. High-pressure-limit rate parameters. [b] BB1K barriers in parentheses.

TABLE 4: Entropy ($S°_{298}$) and Heat Capacity ($C_p(T)$) Values for All Transition States Considered in the Thermal Decomposition of *o*-QM, at the B3LYP/6-311G(2d,d,p) Level[a]

transition state	$S°_{298}$	C_p(300)	C_p(400)	C_p(500)	C_p(600)	C_p(800)	C_p(1000)	C_p(1500)
TS1	77.03	25.16	33.32	40.23	45.82	53.96	59.49	67.37
TS2	81.29	27.19	35.24	41.82	46.97	54.29	59.22	66.46
TS3	81.42	27.48	35.39	41.85	46.93	54.21	59.15	66.42
TS4	79.17	25.65	33.45	40.18	45.70	53.84	59.40	67.34
TS5	82.72	28.68	35.96	41.98	46.85	54.15	59.32	67.05
TS6	81.23	27.58	35.13	41.44	46.54	54.09	59.36	67.14
TS7	81.33	26.63	34.34	40.90	46.25	54.17	59.61	67.43
TS8	85.62	29.49	37.01	43.05	47.83	54.87	59.83	67.27
TS9	82.77	27.80	35.57	41.91	46.95	54.33	59.47	67.11
TS10	80.43	26.25	34.13	40.75	46.09	53.89	59.27	67.12
TS11	80.04	26.12	34.21	40.90	46.21	53.92	59.23	67.02
TS12	82.33	27.10	34.82	41.27	46.44	54.03	59.29	67.06

[a] Transition-state numbering corresponds to that of Table 3 and Figures 2−5. All values in units of cal mol^{-1} K^{-1}.

SCHEME 4: Formation of Tropone from *o*-QM, via 2-Hydroxyphenylcarbene

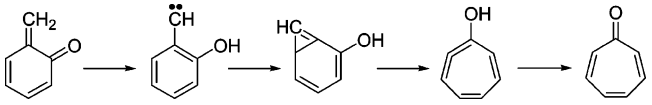

SCHEME 5: Formation of Tropone from *o*-QM, via Ring Opening to 1,3,5,6-Heptatetraen-1-one

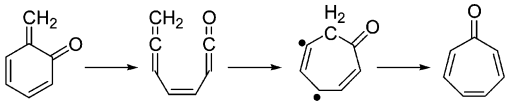

(benzoxete). Benzoxete has now been shown to isomerize with *o*-QM, from both experiment and theory.[22] However, we identify a transition state (TS1, Figure 1) connecting *o*-QM and 2-hydroxyphenylcarbene in a concerted process that does not proceed via benzoxete. A transition state for the benzoxete → 2-hydroxyphenylcarbene reaction could not be located using either the CBS-QB3 or BB1K/6-31+G(2d,p) methods.

It is also plausible that *o*-QM decomposition is initiated via ring opening, as shown in Scheme 5. In this reaction scheme *o*-QM opens to 1,3,5,6-heptatetraen-1-one. This ring opening product cyclizes to the seven-membered (cyclic) diradical 3,6-cycloheptadien-1-one-3,5-yl, and an intramolecular hydrogen shift then produces tropone. We also initially considered an intramolecular hydrogen shift from the CH_2 moiety in 1,3,5,6-heptatetraen-1-one, giving tropone in a concerted process; however, the barrier for this reaction is prohibitively large (ca. 100 kcal mol^{-1} above *o*-QM), and this reaction is therefore not considered important. The cyclic diradical formed upon ring closing should be relatively stable, due to resonance between the depicted 3,6-cycloheptadien-1-one-3,5-yl form and the 3,5-cycloheptadien-1-one-3,7-yl form. Furthermore, there should be a third resonance structure, the 1,3,5-cycloheptatrien-3-yl-1-oxyl diradical; this structure should provide a minor contribution, as we observe with the resonantly stabilized phenoxy and vinoxy radicals, which both prefer the carbonyl (C═O) geometry over the resonance form of the oxyl-type (C−O•) geometry.[23,24] Note

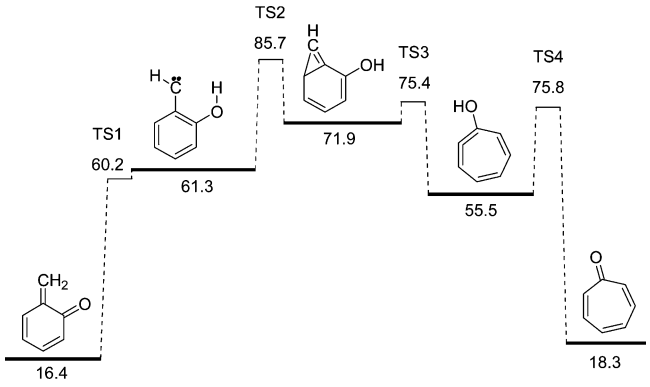

Figure 2. Potential energy diagram for the formation of tropone from *o*-QM, via 2-hydroxyphenylcarbene. Enthalpies of formation in kilocalories per mole.

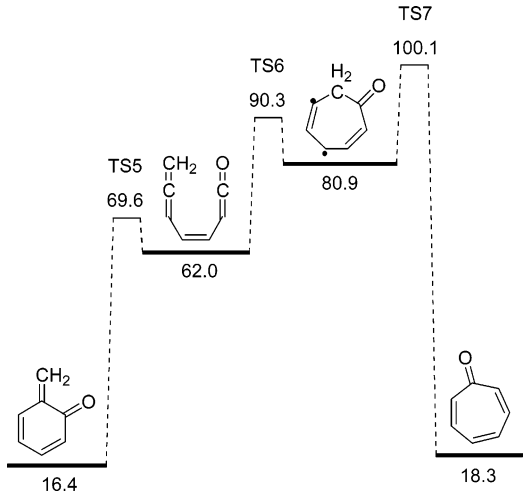

Figure 3. Potential energy diagram for the formation of tropone from *o*-QM, via ring opening. Enthalpies of formation in kilocalories per mole.

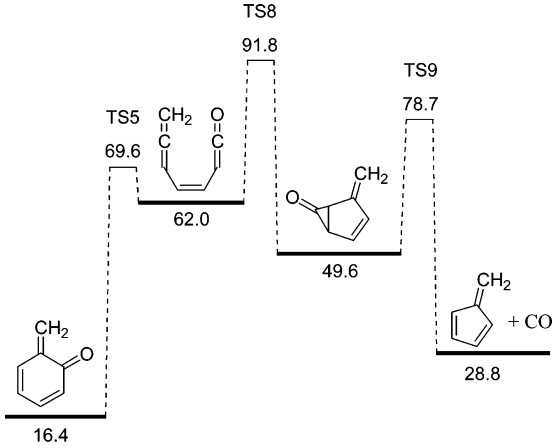

Figure 4. Potential energy diagram for the formation of fulvene from *o*-QM, via ring opening and subsequent closing to 4-methylene-bicyclo-[3.1.0]hex-2-en-6-one. Enthalpies of formation in kilocalories per mole.

that the ring opening product can also undergo a hydrogen-shift reaction to 2,4-heptadien-6-yn-1-one, which may react further to benzene + CO. While this species is of sufficiently low energy ($\Delta_f H° = 96.6$ kcal mol^{-1}), the barrier for the hydrogen-shift reaction from 1,3,5,6-heptatetraen-1-one exhibits a barrier ca. 97 kcal mol^{-1} above the reactant (*o*-QM), making this reaction energetically prohibitive.

A minor product of *o*-QM pyrolysis at low temperatures is fulvene, and this product is considered in our kinetic modeling.

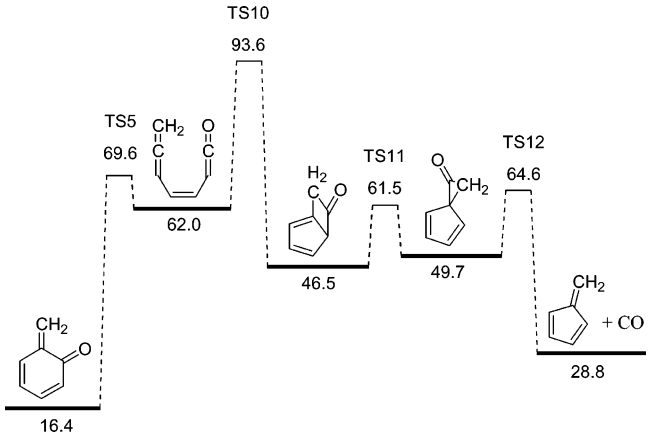

Figure 5. Potential energy diagram for the formation of fulvene from *o*-QM, via ring opening and subsequent closing to bicyclo[3.2.0]hepta-3,5-dien-1-one. Enthalpies of formation in kilocalories per mole.

SCHEME 6: Formation of Fulvene from *o*-QM via 4-Methylenebicyclo[3.1.0]hex-2-en-6-one Dissociation

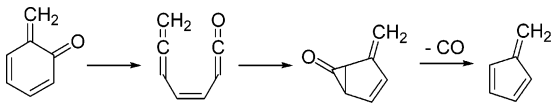

SCHEME 7: Formation of Fulvene from *o*-QM via Spiro[2.4]hepta-4,6-dien-1-one Dissociation

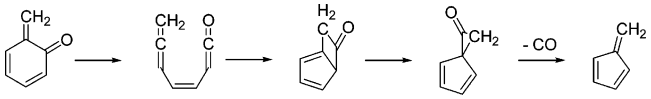

Skokov et al.[4] presented a pathway for the formation of fulvene + CO from *o*-QM, which proceeded via initial ring opening to 1,3,5,6-heptatetraen-1-one. This reaction process is depicted in Scheme 6. Following ring opening, 1,3,5,6-heptatetraen-1-one cyclizes to a bicyclic intermediate (4-methylenebicyclo[3.1.0]-hex-2-en-6-one), which loses CO to provide fulvene.

Finally, we consider the mechanism for fulvene (+CO) formation shown in Scheme 7. This reaction scheme follows the same initial ring opening reaction depicted in Schemes 5 and 6. Following this, the ring opening product cyclizes to the bicyclic intermediate bicyclo[3.2.0]hepta-3,5-dien-1-one, which rearranges to yield spiro[2.4]hepta-4,6-dien-1-one. This intermediate subsequently dissociates to fulvene + CO.

Thermochemical Properties. Table 1 lists the name and structure of each species proposed in the above reaction processes. Also included are enthalpies of formation calculated with the CBS-QB3 method using atomization reactions. Where available, literature enthalpies are also provided (at 298 K). For CO, which is not included in the table, we use a literature enthalpy of formation of −26.417 kcal mol^{-1}.[26]

Entropy and heat capacity values are calculated for all molecules and are presented in Table 2. For bicyclo[4.1.0]hepta-2,4,7-trien-2-ol and 1,2,4,6-cycloheptatetraen-1-ol we considered motion about the R−OH bond as an internal rotor, and not as a vibrational frequency. Internal rotor potentials for these molecules were calculated at the B3LYP/6-31G(d) level and fit to five-parameter Fourier series expansions (see Supporting Information). The mathematical descriptions of the R−OH internal rotors were then used in the program ROTATOR[27] to evaluate the contributions to entropy and heat capacity, which we added to the translational and vibrational components calculated using SMCPS. The SMCPS analyses for these molecules omitted the torsion vibration frequency corresponding

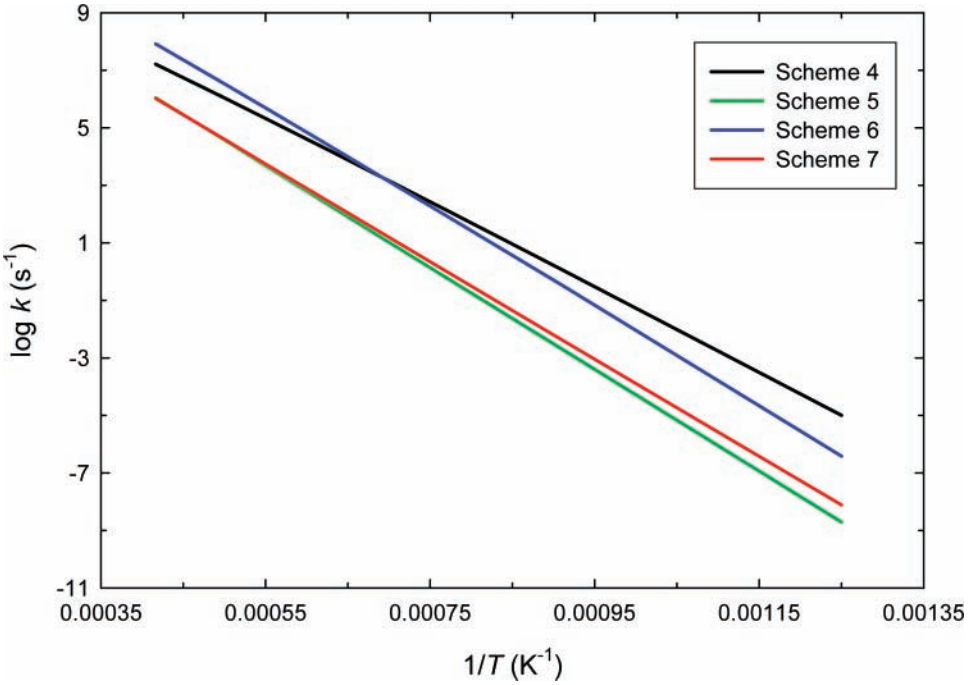

Figure 6. Rate constants as a function of temperature for the thermal decomposition of *o*-QM via the four proposed reaction schemes, using BB1K barrier heights ($P = 1$ atm).

to rotation about the OH group. Internal rotor potentials were also determined for rotation about the R−OH and R−CH bonds in 2-hydroxyphenylcarbene, but the barrier heights were deemed too large (ca. 10 and 16 kcal mol^{-1}, respectively) for these modes to act as hindered internal rotations.

For 2-hydroxyphenylcarbene we identified four stable conformers, one with both the OH and CH groups trans ($\Delta_f H° =$ 63.7 kcal mol^{-1}), one with both groups cis ($\Delta_f H° =$ 69.7 kcal mol^{-1}), one with the OH group trans and the CH group cis ($\Delta_f H° =$ 73.0 kcal mol^{-1}), and a final conformer with the OH group cis and the CH group trans ($\Delta_f H° =$ 61.3 kcal mol^{-1}). The transition state which we identified connecting *o*-QM with 2-hydroxyphenylcarbene results in formation of the most stable conformation (cis−trans), and this is the only conformer considered in this study. This simplification is justified when one considers that the three conformers of 2-hydroxyphenylcarbene are all relatively close in energy ($\Delta_f H° =$ 61.3−73.0 kcal mol^{-1}) and demonstrate similar barrier heights for the forward reaction to bicyclo[4.1.0]hepta-2,4,7-trien-2-ol (around 70−75 kcal mol^{-1} above *o*-QM).

Rate Parameters. Transition states connecting each of the ground-state species have been identified, and their geometries are depicted in Figure 1. The reaction corresponding to each transition state is documented in Table 3. Entropies and heat capacities have been calculated for the transition states from B3LYP/6-311G(2d,d,p) geometries and frequencies, and these values are provided in Table 4. For TS2 and TS3 we modeled the R−OH internal rotor using the entropy and heat capacity corrections evaluated for bicyclo[4.1.0]hepta-2,4,7-trien-2-ol, according to the procedure described above. Using transition-state theory, rate constants were calculated as a function of temperature, which were then fit to empirical rate parameters A' and n, and these values are listed in Table 3. Included in Table 3 are the BB1K barrier heights. There is generally good agreement between the CBS-QB3 and BB1K values (1.6 kcal mol^{-1} average difference).

Potential Energy Diagrams. The potential energy diagram for tropone formation from *o*-QM via a hydroxyphenylcarbene intermediate is shown in Figure 2. The reaction leading to formation of the carbene intermediate is barrierless at the CBS-QB3 level of theory, with the transition state lying 1.1 kcal mol^{-1} below the reaction products. The largest barrier above *o*-QM (69.3 kcal mol^{-1}) is provided by the subsequent rearrangement of 2-hydroxyphenylcarbene to give bicyclo[4.1.0]-hepta-2,4,7-trien-2-ol (TS2). The further reactions of bicyclo-[4.1.0]hepta-2,4,7-trien-2-ol leading to tropone all progress with relatively small barriers, and once formed, a large proportion of this chemically activated adduct should proceed to form tropone. In our kinetic analysis of this reaction scheme we treat the first reaction as the direct formation of bicyclo[4.1.0]hepta-2,4,7-trien-2-ol from *o*-QM through TS2, with an activation energy of 69.3 kcal mol^{-1} (67.1 kcal mol^{-1} at BB1K), due to the negligible barrier for 2-hydroxyphenylcarbene formation.

Figure 3 illustrates the reaction processes involved in tropone formation via initial ring opening. The activation energy for ring opening is smaller than that required for 2-hydroxyphenylcarbene formation. However, this reaction is followed by subsequent reactions with increasingly high barriers, the final barrier being ca. 84 kcal mol^{-1} above the reactant (*o*-QM).

Next, we present the potential energy diagram for fulvene + CO formation via ring opening in *o*-QM, with subsequent closing to 4-methylenebicyclo[3.1.0]hex-2-en-6-one (Figure 4). The largest barrier to reaction is provided by the initial ring opening step, followed by the ring closing reaction leading to 4-methylenebicyclo[3.1.0]hex-2-en-6-one, with respective CBS-QB3 barriers of ca. 53 and 30 kcal mol^{-1}. Once formed, 4-methylenebicyclo[3.1.0]hex-2-en-6-one should dissociate to fulvene + CO as the dominant pathway.

The final potential energy diagram is for formation of fulvene + CO by initial ring opening of *o*-QM, followed by ring closing to bicyclo[3.2.0]hepta-3,5-dien-1-one (Figure 5). In this series of reactions the largest barrier is again provided by ring opening, while the barrier for the subsequent cyclization reaction is similar to that in the previous two reaction schemes (Figures 3 and 4). After the ring opening product closes to bicyclo[3.2.0]-hepta-3,5-dien-1-one we get a low-energy rearrangement fol-

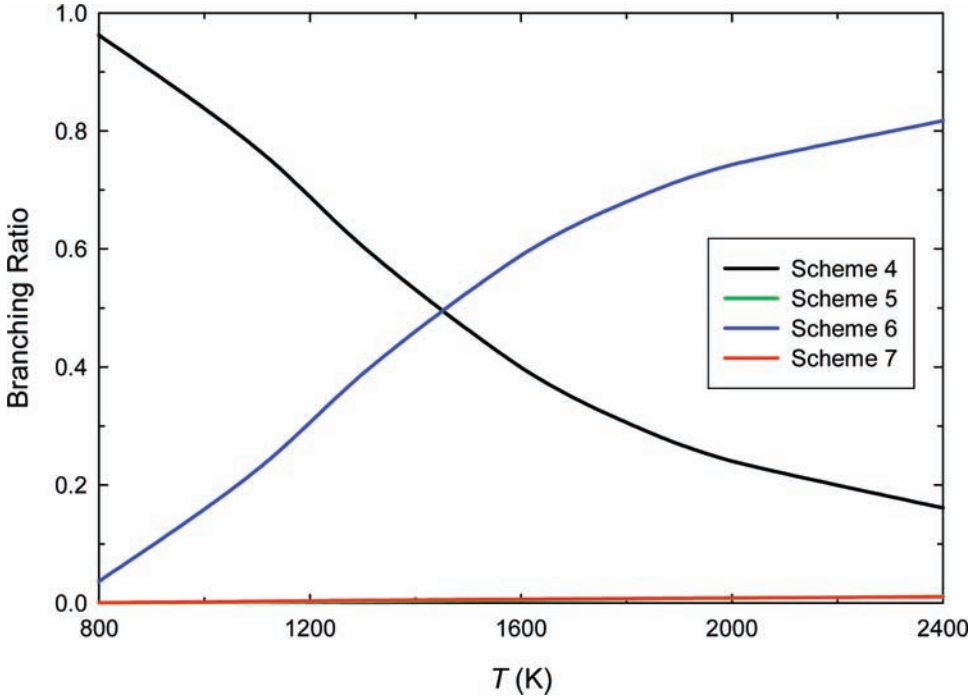

Figure 7. Branching ratios as a function of temperature for the thermal decomposition of *o*-QM via the four proposed reaction schemes, using BB1K barrier heights ($P = 1$ atm). Scheme 5 located under Scheme 7.

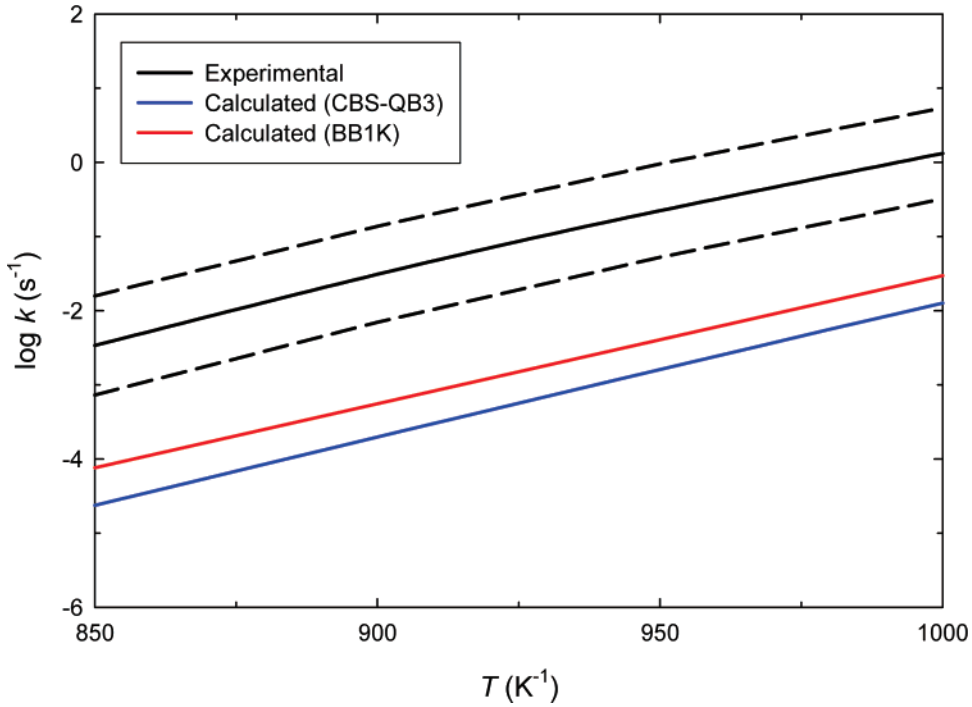

Figure 8. Comparison between experimental and calculated rate constants for the thermal decomposition of *o*-QM at low temperatures. The calculated rate constant corresponds to the sum of the four proposed reaction channels. Dashed lines indicate experimental error margins.

lowed by dissociation to fulvene + CO. As for the previous reaction scheme, the ring closing product (bicyclo[3.2.0]hepta-3,5-dien-1-one) will mostly proceed to fulvene + CO.

Reaction Kinetics. QRRK analysis using the rate parameters presented in Table 3 provides us with rate constants as a function of temperature and pressure for each of the four multistep reaction pathways considered in this study. These rate constants have been tabulated in the Supporting Information. Rate constants for *o*-QM decomposition via the four studied reaction pathways are plotted in Figure 6, as a function of temperature at 1 atm pressure. Branching ratios for the four pathways are illustrated in Figure 7. The results presented in Figures 6 and 7 feature BB1K activation energies, which we next show provide rate constants in better agreement with experiment than the CBS-QB3 values. The formation of tropone (which will dissociate to benzene + CO at even low temperatures) via the 2-hydroxyphenylcarbene reaction pathway dominates at temperatures up to around 1500 K. At higher temperatures the formation of fulvene via Scheme 6 begins to dominate. The remaining reaction pathways are unimportant under all conditions. Around 900 K we find that the minor pathway to fulvene + CO constitutes ca. 10% of the total reaction rate, in agreement with

the experiments of Dorrestijn et al.,[5] which found a benzene to fulvene ratio of 90:10 between 900 and 950 K. These experiments also found that the formation of fulvene became insignificant at temperatures greater than 1040 K, at which point fulvene must rapidly isomerize to the more stable benzene.

Figure 8 shows the predicted rate of *o*-QM pyrolysis (the sum of the four separate reaction channels) at low temperatures, calculated using both CBS-QB3 and BB1K/6-31+G(2d,p) barrier heights. Here, our calculations are compared to an experimental measurement of the rate of *o*-QM decomposition (these experiments were performed in the narrow temperature range of ca. 800−1000 K, and comparison is only made at these temperatures). We find that our predicted rate constants are slower than the experimental result, where the difference is approximately two to three times the quoted error of the experiments. The BB1K results provide a considerably better comparison to the experimental reaction rate, due principally to the lower barrier height for the critical *o*-QM → bicyclo-[4.1.0]hepta-2,4,7-trien-2-ol reaction (67.1 versus 69.3 kcal mol^{-1}).

Our calculated total rate constant using the BB1K barrier heights has been fitted to the Arrhenius equation, yielding $k(T) = 2.64 \times 10^{14} \exp(-35.9/T)$ for $T = 800-2400$ K. This corresponds to an observed activation energy of 71.3 kcal mol^{-1}, compared to the experimental value of 67.2 kcal mol^{-1}.[5] This discrepancy of around 4 kcal mol^{-1} is within the combined error of the calculations and the experiments. It should also be noted that there is good agreement between the calculated and experimental preexponential factors (2.64×10^{14} and 6.31×10^{14} s^{-1}, respectively).

Conclusions

A reaction mechanism for the decomposition of *o*-quinone methide (*o*-QM) to tropone and to fulvene + CO is presented, from quantum chemical calculations. Enthalpies of formation are calculated with the CBS-QB3 theoretical method for all identified species, including transition states, while entropies and heat capacities are evaluated at the B3LYP/6-311G(2d,d,p) level. Barrier heights are also calculated using the BB1K DFT method, which was developed for chemical kinetics. Rate constants at the high-pressure limit for elementary reactions are obtained via conventional transition-state theory, with Wigner tunneling corrections for H-shift reactions. Two reaction pathways are identified leading to tropone, one pathway via an initial hydrogen shift reaction producing 2-hydroxyphenylcarbene and the other pathway via initial ring opening. We also consider two pathways for the formation of fulvene + CO, both via ring opening. Kinetic analysis shows that the formation of tropone (which we expect to decompose further to benzene + CO) through a hydroxyphenylcarbene intermediate dominates *o*-QM decomposition at low to moderate temperatures, with fulvene + CO formation dominating at higher temperatures. The calculated overall rate constant for *o*-QM decomposition is in relatively good agreement with an experimental measurement, where the calculated apparent activation energy is 71.3 kcal mol^{-1}, versus 67.2 kcal mol^{-1} from experiment.

Acknowledgment. This work was supported by the ExxonMobil Educational Fund and the New Jersey Institute of Technology Ada C. Fritts Chair.

Supporting Information Available: CBS-QB3 enthalpies (hartrees), geometries (Cartesian coordinates, Å), frequencies (cm^{-1}), and moments of inertia (atomic units) for all molecules and transition states, R—OH internal rotor potentials for bicyclo-[4.1.0]hepta-2,4,7-trien-2-ol and 1,2,4,6-cycloheptatetraen-1-ol, and $k(T,P)$ for the four studied reaction channels. This material is available free of charge via the Internet at http://pubs.acs.org.

References and Notes

(1) (a) Freccero, M. *Mini-Rev. Org. Chem.* **2004**, *1*, 403. (b) Modica, E.; Zanaletti, R.; Freccero, M.; Mella, M. *J. Org. Chem.* **2001**, *66*, 41.

(2) (a) Toteva, M. M.; Moran, M.; Amyes, T. L.; Richard, J. P. *J. Am. Chem. Soc.* **2003**, *125*, 8814. (b) Weinert, E. E.; Dondi, R.; Colloredo-Melz, S.; Frankenfield, K. N.; Mitchell, C. H.; Freccero, M.; Rokita, S. E. *J. Am. Chem. Soc.* **2006**, *128*, 11940. (c) Zhou, Q.; Turnbull, K. D. *J. Org. Chem.* **2000**, *65*, 2022.

(3) da Silva, G.; Chen, C.-C.; Bozzelli, J. W. *J. Phys. Chem. A*, in press (jp068640x).

(4) Skokov, S.; Kazakov, A.; Dryer, F. L. Fourth Joint Meeting of the U.S. Sections of the Combustion Institute, Philadelphia, PA, Mar 20−23, 2005.

(5) Dorrestijn, E.; Pugin, R.; Ciriano Nogales, M. V.; Mulder, P. *J. Org. Chem.* **1997**, *62*, 4804.

(6) Dorrestijn, E.; Mulder, P. *J. Anal. Appl. Pyrolysis* **1998**, *44*, 167.

(7) Paul, G. C.; Gajewski, J. J. *J. Org. Chem.* **1993**, *58*, 5060.

(8) Dorrestijn, E.; Epema, O. J.; van Scheppinger, W. B.; Mulder, P. *J. Chem. Soc., Perkin Trans. 2* **1998**, 1173.

(9) Eck, V.; Schweig, A.; Vermeer, H. *Tetrahedron Lett.* **1978**, *19*, 2433.

(10) Golden, A. H.; Jones, M., Jr. *J. Org. Chem.* **1996**, *61*, 4460.

(11) Guan, B.; Wan, P. *J. Photochem. Photobiol., A* **1994**, *80*, 199.

(12) Montgomery, J. A., Jr.; Frisch, M. J.; Ochterski, J. W.; Petersson, G. A. *J. Chem. Phys.* **2000**, *112*, 6532.

(13) Ruscic, B.; Pinzon, R. E.; Morton, M. L.; von Laszevski, G.; Bittner, S. J.; Nijsure, S. G.; Amin, K. A.; Minkoff, M.; Wagner, A. F. *J. Phys. Chem. A* **2004**, *108*, 9979.

(14) Sheng, C. Ph. D. Dissertation, New Jersey Institute of Technology, Newark, NJ, 2002.

(15) Frisch, M. J.; Trucks, G. W.; Schlegel, H. B.; Scuseria, G. E.; Robb, M. A.; Cheeseman, J. R.; Montgomery, J. A., Jr.; Vreven, T.; Kudin, K. N.; Burant, J. C.; Millam, J. M.; Iyengar, S. S.; Tomasi, J.; Barone, V.; Mennucci, B.; Cossi, M.; Scalmani, G.; Rega, N.; Petersson, G. A.; Nakatsuji, H.; Hada, M.; Ehara, M.; Toyota, K.; Fukuda, R.; Hasegawa, J.; Ishida, M.; Nakajima, T.; Honda, Y.; Kitao, O.; Nakai, H.; Klene, M.; Li, X.; Knox, J. E.; Hratchian, H. P.; Cross, J. B.; Adamo, C.; Jaramillo, J.; Gomperts, R.; Stratmann, R. E.; Yazyev, O.; Austin, A. J.; Cammi, R.; Pomelli, C.; Ochterski, J. W.; Ayala, P. Y.; Morokuma, K.; Voth, G. A.; Salvador, P.; Dannenberg, J. J.; Zakrzewski, V. G.; Dapprich, S.; Daniels, A. D.; Strain, M. C.; Farkas, O.; Malick, D. K.; Rabuck, A. D.; Raghavachari, K.; Foresman, J. B.; Ortiz, J. V.; Cui, Q.; Baboul, A. G.; Clifford, S.; Cioslowski, J.; Stefanov, B. B.; Liu, G.; Liashenko, A.; Piskorz, P.; Komaromi, I.; Martin, R. L.; Fox, D. J.; Keith, T.; Al-Laham, M. A.; Peng, C. Y.; Nanayakkara, A.; Challacombe, M.; Gill, P. M. W.; Johnson, B.; Chen, W.; Wong, M. W.; Gonzalez, C.; Pople, J. A. *Gaussian 03*, revision D.01; Gaussian, Inc.: Wallingford, CT, 2004.

(16) Wigner, E. P. *Z. Phys. Chem.* **1932**, *B19*, 203.

(17) Zhao, Y.; Lynch, B. J.; Truhlar, D. G. *J. Phys. Chem. A* **2004**, *14*, 2715.

(18) Zheng, J.; Zhao, Y.; Truhlar, D. G. *J. Chem. Theory Comput.* **2007**, *3*, 569.

(19) Chang, A. Y.; Bozzelli, J. W.; Dean, A. M. *Z. Phys. Chem.* **2000**, *214*, 1533.

(20) Bozzelli, J. W.; Chang, A. Y.; Dean, A. M. *Int. J. Chem. Kinet.* **1997**, *29*, 161−170.

(21) For example, see: Gasper, P. P.; Hsu, J.-P.; Chari, S. *Tetrahedron* **1985**, *41*, 1479.

(22) Qiao, G. G.; Lenghaus, K.; Solomon, D. H. *J. Org. Chem.* **1998**, *63*, 9806.

(23) da Silva, G.; Kim, C.-H.; Bozzelli, J. W. *J. Phys. Chem. A* **2006**, *110*, 7925.

(24) da Silva, G.; Chen, C.-C.; Bozzelli, J. W. *Chem. Phys. Lett.* **2006**, *424*, 42.

(25) Roth, W. R.; Adamczak, O.; Breuckmann, R.; Lennartz, H.-W.; Boese, R. *Chem. Ber.* **1991**, *124*, 2499.

(26) Chase, M. W., Jr. *J. Phys. Chem. Ref. Data, Monogr.* **1998**, *9*, 1).

(27) (a) Lay, T. H.; Krasnoperov, L. N.; Venanzi, C. A.; Bozzelli, J. W. *J. Phys. Chem.* **1996**, *100*, 8240. (b) Yamada, T.; Lay, T. H.; Bozzelli, J. W. *J. Phys. Chem. A* **1999**, *103*, 5602.